

TABLE 1. Mössbauer parameters for ferric hydroxamates*

| | Pressure (kbar) | | | | | | | | | |
|----------------------|-----------------|-------|-------|-------|-------|-------|-------|-------|--|---------|
| | 4 | 25 | 50 | 75 | 100 | 125 | 150 | 175 | | |
| Fe(SHA) ₃ | | | | | | | | | | |
| Fe(III) | 0.440 | 0.450 | 0.445 | 0.430 | 0.427 | 0.420 | 0.413 | 0.406 | | (23°C) |
| Fe(II) | —† | — | — | 1.36 | 1.35 | 1.34 | 1.33 | 1.32 | | |
| Fe(AHA) ₃ | | | | | | | | | | |
| Fe(III) | 0.415 | 0.414 | 0.414 | 0.411 | 0.410 | 0.403 | 0.393 | 0.381 | | (23°C) |
| Fe(II) | — | — | — | 1.39 | 1.38 | 1.37 | 1.36 | 1.35 | | |
| Fe(BHA) ₃ | | | | | | | | | | |
| Fe(III) | 0.370 | 0.426 | 0.431 | 0.426 | 0.422 | 0.415 | 0.408 | 0.401 | | (23°C) |
| Fe(II) | — | — | — | — | 1.35 | 1.31 | 1.27 | 1.23 | | |
| Ferrichrome A | | | | | | | | | | |
| Fe(III) | 0.195 | 0.265 | 0.390 | 0.410 | 0.394 | 0.370 | 0.350 | 0.335 | | (23°C) |
| Fe(II) | — | — | 1.202 | 1.200 | 1.200 | 1.198 | 1.195 | 1.194 | | |
| Fe(SHA) ₃ | | | | | | | | | | |
| Fe(III) | 0.94 | 1.11 | 1.23 | 1.31 | 1.36 | 1.40 | 1.43 | 1.45 | | (23°C) |
| Fe(II) | — | — | — | 2.29 | 2.20 | 2.17 | 2.15 | 2.14 | | |
| Fe(III) | — | — | 1.26 | 1.30 | 1.42 | 1.47 | 1.51 | 1.53 | | (110°C) |
| Fe(II) | — | — | — | 2.05 | 2.02 | 2.03 | 2.05 | 2.06 | | |
| Fe(III) | — | — | 1.32 | 1.41 | 1.46 | 1.50 | 1.51 | 1.53 | | (135°C) |
| Fe(II) | — | — | 2.08 | 2.04 | 2.06 | 2.09 | 2.12 | 2.14 | | |
| Fe(AHA) ₃ | | | | | | | | | | |
| Fe(III) | 0.70 | 0.99 | 1.13 | 1.21 | 1.25 | 1.28 | 1.30 | 1.33 | | (23°C) |
| Fe(II) | — | — | — | 2.32 | 2.31 | 2.30 | 2.28 | 2.27 | | |
| Fe(III) | — | — | 1.19 | 1.32 | 1.41 | 1.48 | 1.51 | 1.55 | | (135°C) |
| Fe(II) | — | — | — | 1.97 | 1.98 | 2.00 | 2.01 | 2.03 | | |
| Fe(BHA) ₃ | | | | | | | | | | |
| Fe(III) | 0.70 | 0.91 | 1.06 | 1.17 | 1.25 | 1.32 | 1.36 | 1.39 | | (23°C) |
| Fe(II) | — | — | — | — | 2.31 | 2.25 | 2.19 | 2.14 | | |
| Fe(III) | — | 1.06 | 1.18 | 1.27 | 1.36 | 1.42 | 1.47 | 1.48 | | (105°C) |
| Fe(II) | — | — | — | — | 1.99 | 1.98 | 1.97 | 1.97 | | |
| Fe(III) | — | — | 1.06 | 1.17 | 1.25 | 1.32 | 1.36 | 1.39 | | (135°C) |
| Fe(II) | — | — | 1.86 | 1.86 | 1.85 | 1.85 | 1.84 | 1.84 | | |
| Ferrichrome A | | | | | | | | | | |
| Fe(III) | 0.37 | 0.59 | 1.01 | 1.20 | 1.32 | 1.39 | 1.46 | 1.50 | | (23°C) |
| Fe(II) | — | — | 2.49 | 2.44 | 2.42 | 2.40 | 2.40 | 2.39 | | |

* Data given as (mm/sec) isomer shifts (quadrupole splitting) relative to iron metal.

† —, not present.

discussed below, that Fe(BHA)₃ showed markedly more asymmetric peaks than the other two model compounds, indicating some difference in its structure, which might account for the unusual behavior of its isomer shift. However, the fitting of such asymmetric peaks is difficult, and we cannot eliminate the possibility that the peculiar behavior in the low-pressure region is in part an artifact of the fitting. The Fe(III) quadrupole splittings all increased by about 0.6 mm/sec in 175 kbar. The Fe(II) isomer shift of about 1.35 mm/sec, and the large quadrupole splitting of about 2.20 mm/sec, clearly indicates that the Fe(II) produced at high pressure is high spin.

As discussed above, Fe(SHA)₃ showed asymmetric peaks at low pressures, and with increasing pressure the asymmetry decreased. Fe(BHA)₃ showed even greater relaxation effects, and its ratio of peak widths was about 1.56 at 4 kbar, as compared to 1.25 for Fe(SHA)₃. With increasing pressure, the relaxation effect in Fe(BHA)₃ also decreased, and by 70 kbar the ratio was down to 1.09. By 90 kbar, the ratio appeared to be one. Fe(AHA)₃, in contrast to the other two compounds, showed only a small relaxation effect, so the peaks were fit as symmetric at all pressures. This relaxation effect was also

observed in some ferric hydroxamates studied by Epstein *et al.* (13). They found that Fe(AHA)₃ and Fe(SHA)₃ showed modest relaxation effects, while Fe(BHA)₃ exhibited a much larger effect. The asymmetry is associated with the relative population of ground and excited nuclear states. As the distance between iron sites decreases with increasing pressure, we would expect both an increase in splitting of the levels and a decrease in relaxation time. Both these factors would serve to decrease the asymmetry.

STUDIES WITH FERRICHRROME A

Ferrichrome A was also studied at different pressures, both optically and with Mössbauer resonance. The optical spectrum is very much like that of the model compounds described above. The charge transfer peak is at 22.22 kK, and at 50% of maximum absorption the energy is 18.9 kK. The shift of the charge transfer peak at 50% of maximum absorption is 1.5 kK to lower energy, some 0.25 kK larger than the shifts in the model compounds.

The Mössbauer spectra of ferrichrome A at 4 kbar and 138 kbar is shown in Fig. 5. Note that the lower-pressure spectrum is broadened considerably more than the model compound

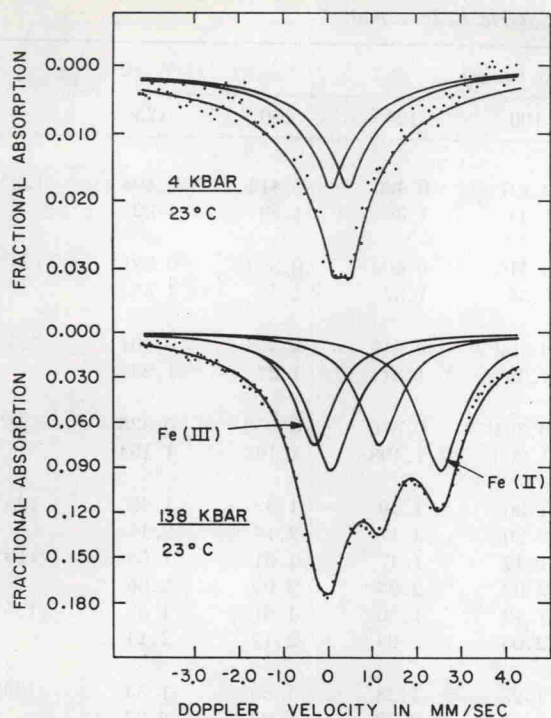
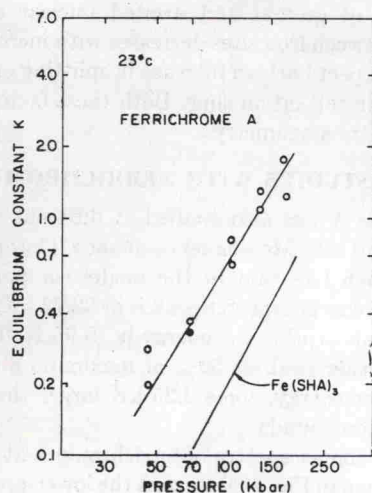


Fig. 5. Mössbauer spectra of ferrichrome A.

Fe(SHA)₃ shown in Fig. 2. This broadening in ferrichrome A has been attributed by Wickman *et al.* (14) to the presence of a magnetic hyperfine structure. At room temperature, the hyperfine interaction is produced by a field having a shorter relaxation time than at low temperatures, and the hyperfine interaction dissolves into the broad line shown. For comparison to the model compounds, the spectra were fit as a quadrupole split pair at low pressure. At high pressure, the iron of ferrichrome A was also reduced, in greater yields than in the model compounds, as shown in Fig. 6, where the conversion of the ferrichrome at 23°C is compared to that of Fe(SHA)₃. Ferrichrome A was not run at higher temperatures because of the possibility of decomposition. The Fe(II) produced is also high spin, with an isomer shift of about 1.2

Fig. 6. $\ln K$ vs. $\ln P$ for ferrichrome A.TABLE 2. Parameters A and B for $K = AP^B$

| Compound | T(°C) | A | B | Pressure range (kbar) |
|----------------------|-------|-----------------------|------|-----------------------|
| Fe(SHA) ₃ | 23 | 3.66×10^{-5} | 1.86 | 60-170 |
| | 110 | 6.64×10^{-7} | 3.03 | 50-150 |
| | 135 | 1.45×10^{-7} | 3.62 | 40-110 |
| Fe(BHA) ₃ | 23 | 8.08×10^{-7} | 2.54 | 100-175 |
| | 105 | 2.35×10^{-5} | 2.03 | 90-175 |
| | 135 | 3.96×10^{-4} | 1.66 | 60-175 |
| Fe(AHA) ₃ | 23 | 1.30×10^{-3} | 0.94 | 100-175 |
| | 135 | 4.19×10^{-4} | 1.60 | 55-175 |
| Ferrichrome A | 23 | 3.12×10^{-4} | 1.67 | 40-175 |

mm/sec. The isomer shift and quadrupole splitting of both Fe(III) and Fe(II) in ferrichrome A are given in Table 1, and the parameters A and B are given in Table 2 for all the ferric hydroxamates. Values of the parameters for ferrichrome should be considered as somewhat qualitative since the spectra were broadened by the hyperfine interaction.

The reduction of ferric iron to ferrous iron requires a transfer of an electron from the ligands to the metal. As previously mentioned, the charge transfer energies for Fe(AHA)₃, Fe(BHA)₃, and Fe(SHA)₃ are 23.25, 22.22, and 21.95 kK, respectively. Referring back to Fig. 4, we can see that this is also the order of increasing conversion, so there is a definite correlation between the energy of the charge transfer band and the amount of conversion observed in a series of closely similar compounds. This is entirely consistent with our theory presented previously (15, 16), in which we suggested that the reduction occurred because the excited state (the Fe(II) plus ligands with a hole) decreases in energy with respect to the ground state (Fe(III) ion plus normal ligands) with increasing pressure, until a thermal transfer of an electron becomes possible. Because of the Franck-Condon principle, the optical transfer of an electron occurs vertically on a configuration coordinate diagram in contrast to the thermal process, as shown in Fig. 7. Nevertheless, the correlation between optical and thermal processes might be expected as long as the shapes of the potential wells are very similar from

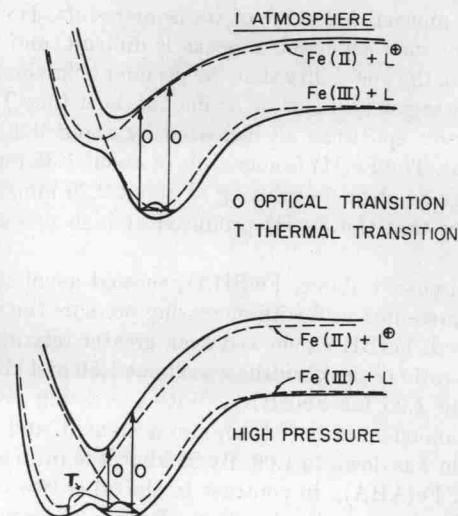


Fig. 7. Schematic configuration coordinate diagram.